Microchimica Acta (2024) 191:384
https://doi.org/10.1007/s00604-024-06456-4

ORIGINAL PAPER

Multifunctional N, Fe-doped carbon dots with peroxidase-like activity for the determination of H_2O_2 and ascorbic acid and cell protection against oxidation

Shenna Chen[1] · Ronghui Li[1] · Bo Zhao[2] · Mei Fang[1] · Yun Tian[3] · Yuhua Lei[3] · Yayong Li[4] · Lina Geng[1]

Received: 2 April 2024 / Accepted: 21 May 2024 / Published online: 11 June 2024

Abstract

Multifunctional N, Fe-doped carbon dots (N, Fe-CDs) were synthesized by the one-step hydrothermal method using ferric ammonium citrate and dicyandiamide as raw materials. The N, Fe-CDs exhibited peroxidase-like (POD) activity by catalyzing the oxidization of 3,3′,5,5′-tetramethylbenzidine (TMB) to the green oxidation state ox-TMB in the presence of hydrogen peroxide (H_2O_2). Subsequently, based on the POD activity of N, Fe-CDs, an efficient and sensitive colorimetric method for the detection of H_2O_2 and ascorbic acid (AA) was established with a limit of detection of 0.40 μM and 2.05 μM. The proposed detection method has been successfully applied to detect AA in fruit juice, vitamin C tablets, and human serum samples and has exhibited excellent application prospects in biotechnology and food fields. Furthermore, N, Fe-CDs also showed a protective effect on the cell damage caused by H_2O_2 and could be used as an antioxidant agent.

Keywords N, Fe-codoped carbon dots · Peroxidase-like activity · Colorimetric detection · H_2O_2 · Ascorbic acid

Introduction

As a kind of natural enzyme, peroxidase is widely applied in the chemical industry, biomedicine, and environmental science and food fields [1]. Unfortunately, natural peroxidases have shortcomings, such as instability, high production cost, and high conditions [2]. Accordingly, the preparation and application development of artificial peroxides are significant and urgent works.

Nanozyme as an artificial peroxide has the advantages of high stability, low cost, and simple preparation and is widely applied to biomolecular measurement and environmental protection [3]. Pt nanoparticles, gold clusters, carbon dots, graphene oxide, V_2O_5 nanowires, and CuS clews have been proven to have peroxide-like (POD) activities, similar to natural horseradish peroxidase (HRP) [4]. Among them, carbon dots (CDs) have received extensive concern because of their advantage of small size, large specific surface area, excellent catalytic efficiency, and strong substrate specificity [5]. The POD activity of CDs could be measured by the color reaction that the oxidation of 3,3′,5,5′-tetramethylbenzidine (TMB) was catalyzed by CDs in the presence of hydrogen peroxide (H_2O_2). The color change is directly affected by the content of H_2O_2, and the oxidation of TMB can be inhibited by reducing substances, such as ascorbic acid, which are the basis for establishing detection methods based on the POD activity of CDs.

H_2O_2 is an important signaling molecule in cell differentiation, disease progression and biological systems [6]. However, excessive H_2O_2 will pollute the environment, cause severe damage to cells, and even lead to apoptosis [7]. Ascorbic acid (AA, vitamin C) is an essential water-soluble vitamin and a potent reducing agent, which plays a vital role in many physiological processes [8]. In addition, AA was also extensively used in food, skin care products, and healthcare products. Therefore, the accurate and effective determination of H_2O_2 and AA were of great significance to human health,

✉ Lina Geng
genglina0102@126.com

[1] Hebei Technology Innovation Center for Energy Conversion Materials and Devices, College of Chemistry and Material Science, Hebei Normal University, Shijiazhuang 050024, P. R. China

[2] Experimental Center for Teaching, Hebei Medical University, Shijiazhuang 050017, P. R. China

[3] College of Basic Medicine, Hebei Medical University, Shijiazhuang 050017, P. R. China

[4] Department of Rehabilitation Medicine, Shijiazhuang People's Hospital, Shijiazhuang 050000, P. R. China

environmental monitoring, and food safety. In addition, how to reduce or eliminate the damage of H_2O_2 to cells was also an urgent problem that needed to be solved.

There are a series of analytical methods for AA and H_2O_2 sensing, including fluorescence, electrochemistry, chemiluminescence, chromatography, capillary zone electrophoresis, and colorimetry [9–11]. However, more accessible and effective strategies for detecting AA and H_2O_2 are still in demand. Colorimetry was completely facile, rapid, straightforward, stable, and repeatable among these developed methods.

In this study, we prepared multifunctional N, Fe-doped carbon dots (N, Fe-CDs) with peroxidase-like (POD) activity for detecting H_2O_2 and AA and protecting the peroxidation of smooth muscle cells damaged by H_2O_2. The oxidation of TMB (3,3′,5,5′-tetramethylbenzidine) in the presence of H_2O_2 and N, Fe-CDs has proven the POD activity of N, Fe-CDs. Based on the change of absorbance and color, an economical and convenient colorimetric detection platform for both H_2O_2 and AA has been constructed. The AA content in serum, fruit juice, and vitamin C tablets was determined, indicating the reliability of the sensing method in the biochemistry and diagnosis fields. The smooth muscle cells damaged by H_2O_2 recovered to a certain extent, illustrating the protective effect of N, Fe-CDs on H_2O_2-injured cells.

Experimental

Materials and reagents

Materials and reagents are provided in the electronic supplementary material (ESM).

Preparation of N, Fe-CDs

Ferric ammonium citrate and dicyandiamide were weighed at a molar ratio of 1:1, dissolved in 8 mL distilled water, transferred to a high-pressure reaction kettle, and heated at 180 ℃ for 10 h. The reactor was naturally cooled to room temperature. After filtration, centrifugation, and dialysis purification, the brown N, Fe-CDs solution was obtained. The powder sample was obtained by drying N, Fe-CDs solution in a drying oven at 85 ℃ and stored at 4 ℃ for later use. Before the experiment, the powder was dissolved into a specific concentration of N, Fe-CDs solution with distilled water.

Multifunctional study of N, Fe-CDs based on the POD activity

Colorimetric determination of H_2O_2 and AA

N, Fe-CDs (0.2 mL, 0.1 mg·mL^{-1}), TMB (0.1 mL, 3 mM), 1.6 mL NaAc-HAc buffer (0.2 M, pH 3.6), and 0.1 mL of different concentration of H_2O_2 were mixed at room temperature for 15 min. The characteristic absorbance of ox-TMB at 652 nm was measured to detect H_2O_2.

In the following AA detection experiment, TMB (0.1 mL, 3 mM), H_2O_2 (0.1 mL, 10 mM), and N, Fe-CDs (0.2 mL, 0.1 mg·mL^{-1}) were added to 1.6 mL NaAc-HAc buffer solution for 15 min, and then AA was added. The final concentration of AA in the reaction system was 5 to 100 μM, and then the absorbance at 652 nm was measured by UV-Vis spectra.

The practical samples were analyzed to evaluate the practicality and feasibility of the AA detection method. The vitamin C tablets were purchased from the local pharmacy, dissolved in distilled water, and then diluted to a suitable concentration. The serums were provided by three healthy volunteers and stored at − 4 ℃ before use. Initially, the serum samples were diluted 100 times with NaAc-HAc buffer. The AA content in the actual samples was determined according to the above AA detection assay.

The protective effect of N, Fe-CDs on peroxidation of vascular smooth muscle cells damaged by H_2O_2

CCK-8 assays were used to determine cell viability. Vascular smooth muscle cells (VSMCs) were seeded into a 96-well plate (7×10^3 cells/well) and cultured in Dulbecco's modified Eagle's medium (DMEM) at 37℃ for 24 h. Then, the cells were treated with various concentrations of CDs (25, 50, and 100 μg/mL) with or without H_2O_2 (500 μmol/L) for 24 h. Finally, cell viability was detected using a CCK-8 kit according to the manufacturer's instructions. CCK-8 was added to each well after culturing, and then the cells were incubated for 3 h at 37 ℃ prior to measurement. The absorbance at 450 nm was detected using a microplate reader.

Results and discussion

Characterization of N, Fe-CDs

N, Fe-CDs were prepared from ferric ammonium citrate and dicyandiamide using a one-pot hydrothermal method. The morphology of the N, Fe-CDs was characterized by TEM. TEM image showed that the N, Fe-CDs were spherical particles with an average size of 4.5 ± 1.58 nm and exhibited good dispersion (Fig. 1A). The phase and structure of as-prepared N, Fe-CDs were characterized by XRD. XRD pattern showed a broad peak at around $2\theta = 23°$ (Fig. 1B), corresponding to the amorphous carbon phase [12]. The surface functional groups and elemental composition were characterized by the FT-IR and XPS spectrums. FT-IR spectrum of N, Fe-CDs displayed characteristic absorption bands (Fig. 1C). The absorption peaks at 3431 and 3212 cm^{-1} were

O-H and N-H stretching vibration [13]; the absorption peak at 1621 cm^{-1} was C = O/C = N stretching vibration [14]; the absorption peaks at 1398 cm^{-1} and 1061 cm^{-1} correspond to the stretching vibrations of C-N and C-O [15], respectively; the absorption peak at 851 cm^{-1} correspond to = C-H [16]. These results indicated the presence of O- with N-containing groups. The peak at 635 cm^{-1} was attributable to the Fe-O stretching vibration in N, Fe-CDs [17], which suggested that the iron element was successfully doped into CDs.

XPS characterization was a powerful method for analyzing the surface functional groups and chemical composition of N, Fe-CDs. As shown in Fig. 1D, the full survey

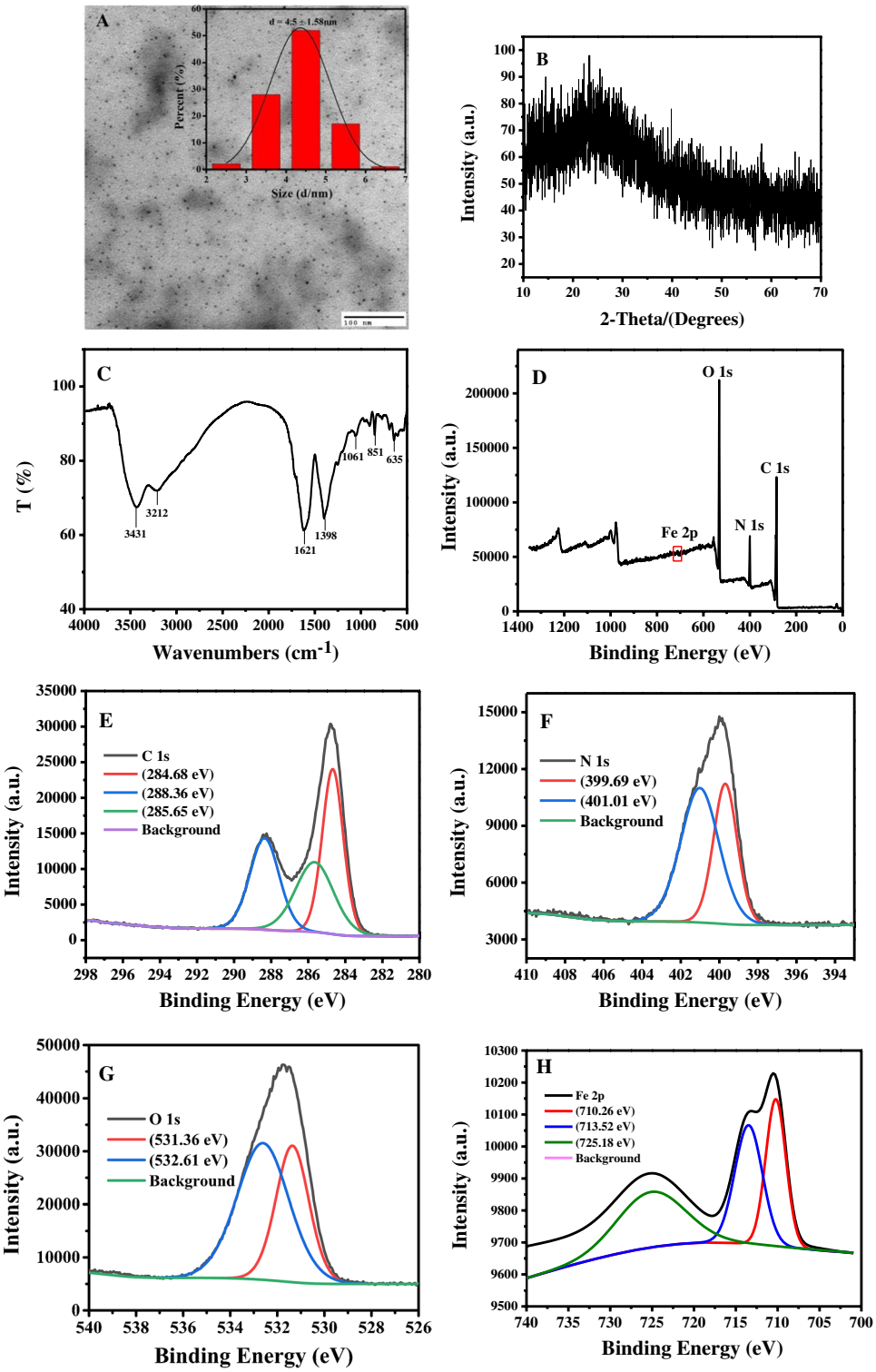

Fig. 1 Characterization of N, Fe-CDs: **A** TEM image and particle size distribution (inset); **B** PXRD pattern; **C** FT-IR spectrum; **D** XPS full survey; **E** C 1s spectra, **F** N 1s spectra, **G** O 1s spectra; and **H** Fe 2p spectra

spectrum of N, Fe-CDs exhibited three typical peaks at 285 eV, 400 eV, and 532 eV, which belonged to C 1s, N 1s, and O 1s, respectively. In addition, there was a small peak at 172 eV corresponding to Fe 2p. In the high-resolution C 1s spectrum (Fig. 1E), the peaks at 284.68 eV, 285.65 eV, and 288.36 eV were attributed to C = C, C-C, and C-N-C, respectively. The N 1s spectrum (Fig. 1F) was fitted into two peaks at 399.69 eV (C-N) and 401.01 eV(C-N-H), respectively. Two peaks in the O 1s spectrum (Fig. 1G) at 531.36 eV and 532.61 eV were assigned to C-OH/C-O-C and C = O groups, respectively. The Fe 2p of N, Fe-CDs (Fig. 1H and Fig. S1) showed three peaks at 710.26 eV, 713.52 eV, and 725.18 eV, attributed to Fe^{2+} $2p_{3/2}$, Fe^{3+} $2p_{3/2}$, and Fe^{3+} $2p_{1/2}$, respectively [13, 17]. Due to the low-resolution problem, the peak of Fe^{2+} $2p_{1/2}$ (around 721 eV) could not be found. These results suggested that N, Fe-CDs were composed of carbon, nitrogen, oxygen, and iron and the nitrogen and iron elements were successfully incorporated into the CDs.

The optical properties of N, Fe-CDs were characterized by fluorescence and UV-Vis spectra. Fig. S1A showed the UV-Vis absorption spectra of N, Fe-CDs, two absorption peaks at 240 nm and 340 nm, which were attributed to the π-π* electron transition of C = C and the n-π* electron transition of C = O/C = N, respectively [18]. The optimal excitation and emission peaks of N, Fe-CDs were symmetrical and located at 350 nm and 440 nm, respectively. The emission spectrum of N, Fe-CDs was independent of the excitation wavelength when the excitation wavelength changed from 320 to 380 nm, and the highest fluorescent intensity was obtained when the excitation wavelength was 350 nm (Fig. S1B). Color coordinates showed that N, Fe-CDs emitted blue light under ultraviolet irradiation (Fig. S1A inset).

The POD activity of the N, Fe-CDs

The POD activity of N, Fe-CDs was evaluated using TMB as a catalytic oxidation substrate in the presence of H_2O_2. Figure 2 shows the UV-Vis spectra and corresponding photographs. The TMB solution was colorless and showed no evident absorbance peak. However, the TMB + H_2O_2 + N, Fe-CDs solution exhibited a visible green color change and a significant absorbance peak at 652 nm, indicating that ox-TMB (the oxidation product of TMB) was generated. These results suggested that N, Fe-CDs have POD activity and can catalyze the oxidation of TMB to ox-TMB by H_2O_2.

The effects of N, Fe-CDs concentration, TMB concentration, H_2O_2 concentration, pH, temperature, and NaCl concentration on the catalytic performance of N, Fe-CDs were investigated in Fig. S2.

The absorbance of ox-TMB at 652 nm gradually increased with the increase of the N, Fe-CDs concentration and reaction time. Under the premise of ensuring the POD activity, to save the carbon dots and time, we selected 10 μg/mL of N, Fe-CDs and 15 min for the following experiments. With the increase of TMB and H_2O_2 concentration, the enzyme activity increased gradually and then leveled off. With the rise of pH value, the catalytic activity of N, Fe-CDs increased at the beginning and then decreased and reached the maximum value at pH 3.6. In addition, the enzyme activities of N, Fe-CDs at a range of temperatures (4–55℃) and concentrations of salt solution (0–300 mM) were investigated. N, Fe-CDs can maintain more than 60% enzyme activity at a low temperature of 4 ℃ and a high temperature of 55 ℃. The POD activity of the carbon dots has good stability under physiological conditions. Furthermore, N, Fe-CDs powder was stored at 4℃ for half a year, and the fluorescence properties and POD activity of N, Fe-CDs solution were not affected and can be used normally, indicating the long-term stability of N, Fe-CDs. Therefore, The maximum catalytic activity was thus obtained under the following conditions: pH 3.6 (0.2 M of NaAc-HAc buffer), 25 ℃, 15 min, 0.15 mM of TMB, 0.5 mM of H_2O_2, and 10 μg/mL of N, Fe-CDs.

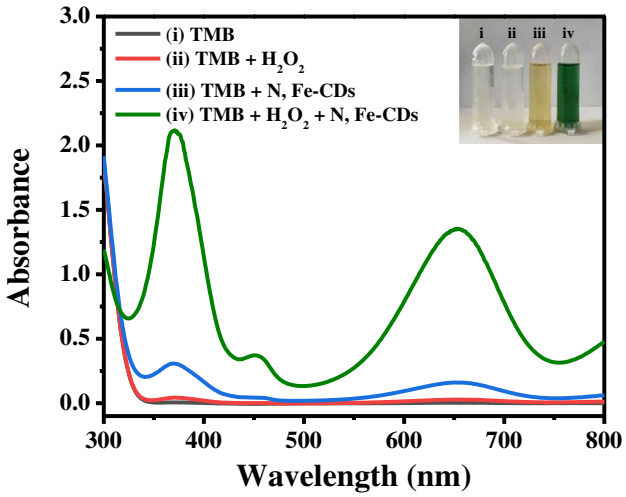

Fig. 2 Absorption spectra of TMB solution (i) and in the presence of H_2O_2 (ii), N, Fe-CDs (iii), H_2O_2, and N, Fe-CDs (iv). The inset shows the corresponding photo of the mixture solution. The concentrations of N, Fe-CDs, TMB, and H_2O_2 were 10 μg/mL, 0.15 mM, and 0.5 mM, respectively

Kinetic exploration of POD activity

The Michaelis-Menten curves were used to investigate the POD activities of N, Fe-CDs with H_2O_2 and TMB as substrates under optimized experimental conditions. A univariate method was adapted to change the substrate concentration using reaction rate as the leading evaluation indicator. The catalytic parameters were obtained according to the experimental approach described in Section 2.5. The K_m and V_{max} represent the Michaelis-Menten constant and the maximal reaction velocity calculated from the Lineweaver-Burk

plots. First, the concentration of H_2O_2 was fixed at 0.5 mM, and the concentration of TMB was changed to obtain the typical Michaelis-Menten equation curve and Lineweaver-Burk plots (Fig. 3A). The K_m value of N, Fe-CDs peroxidase was calculated as 0.423 mM and the V_{max} value as 12.15×10^{-8} $M \cdot s^{-1}$. When the concentration of TMB was fixed, and the concentration of H_2O_2 was changed, the typical Michaelis-Menten equation curve and Lineweaver-Burk plots with the concentration of H_2O_2 were obtained (Fig. 3B), and the K_m and V_{max} values were 0.169 mM and 4.99×10^{-8} $M \cdot s^{-1}$, respectively. The K_m and V_{max} values of N, Fe-CDs and corresponding values of other nano-peroxidase-like enzymes in the literature were listed in Table S1. K_m reflected the affinity of the enzyme to the substrate. The greater the K_m value, the weaker the substrate affinity of the enzyme, whereas a higher V_{max} value suggested a higher catalytic activity [19]. The K_m value of N, Fe-CDs with TMB as the substrate was lower as compared to that of HRP, N/Cu-CDs and Cu NCs, indicating that N, Fe-CDs have greater affinity for TMB than those listed above. The K_m value of N, Fe-CDs with H_2O_2 was lower in comparison with those of other nanomaterials except for GQDs/CuO nanocomposite, suggesting that the affinity of N, Fe-CDs for H_2O_2 was higher. In addition, the larger V_{max} value also indicated that N, Fe-CDs have higher catalytic activity than HRP and other enzyme mimics.

By changing the concentrations of the two substrates, the Lineweaver-Burk plots were obtained to study the POD catalytic process of N, Fe-CDs (Fig. 3C and D). The approximate parallel lines were acquired, indicating that the Michaelis-Menten kinetic characteristics of N, Fe-CDs and the peroxide-like activity of N, Fe-CDs conform to the ping-pong mechanism, which suggests that N, Fe-CDs as

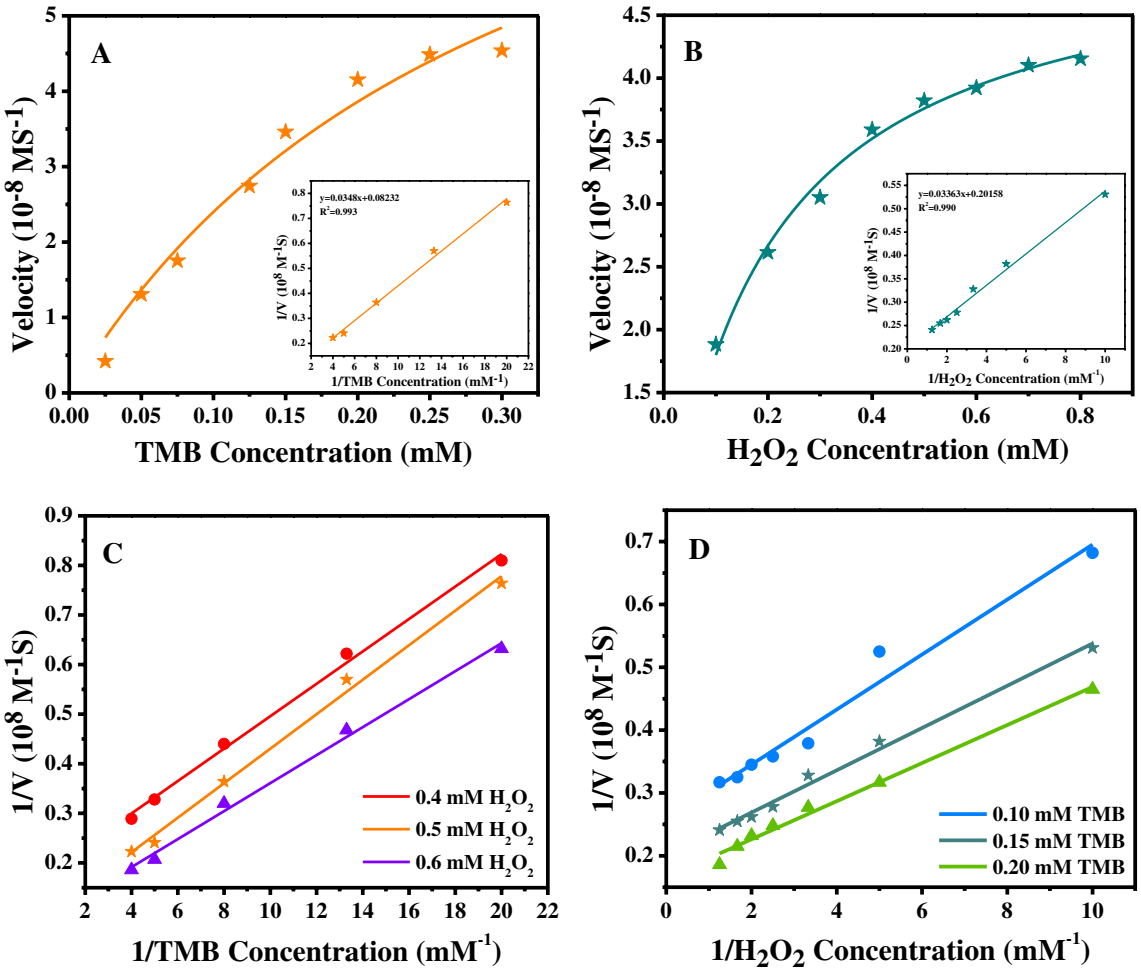

Fig. 3 Steady-state kinetic parameters and catalytic mechanism of N, Fe-CDs. The catalytic reaction velocity was measured by using N, Fe-CDs (10 μg/mL) at 25 °C in NaAc-HAc buffer (0.2 M, pH 3.6). **A** catalytic reaction velocity when H_2O_2 concentration was fixed at 0.5 mM and TMB concentration was changed; **B** catalytic reaction velocity when TMB concentration was fixed at 0.15 mM and H_2O_2 concentration was changed. Insets were the Lineweaver-Burk plots of the double reciprocal of the Michaelis-Menten equation. **C**, **D** Double reciprocal plots of catalytic activity of N, Fe-CDs when the concentration of one substrate (TMB or H_2O_2) was fixed while that of the other was changed

the catalyst bind to and react with the first substrate, generated and released the first product, and then recombined and reacted the second substrate [20].

Mechanism of POD activity of N, Fe-CDs

According to previous reports, the peroxide-like enzyme activity of carbon dots is probably related to the generation of ROS (·OH) [21]. In the EPR experiment, DMPO was used as a trapping agent to verify the formation of hydroxyl radicals during the POD catalytic process of N, Fe-CDs. DMPO can react with ·OH to produce a stable DMPO/·OH, which has a typical four lines EPR signal with a relative intensity of 1:2:2:1. Figure 4A shows the results of the EPR experiment; the EPR signals of N, Fe-CDs, H_2O_2, and N, Fe-CDs + H_2O_2 mixed with DMPO were detected respectively. It was found that only the reaction system of N, Fe-CDs + H_2O_2 generated ·OH signal (1:2:2:1). This indicated that active intermediates (·OH) were generated in the catalytic process with N, Fe-CDs as peroxidase.

In addition, according to previous literature, Rh B was selected as a probe to verify further the production of ·OH in the N, Fe-CDs catalyzed peroxidase reaction [22]. As shown in Fig. 4B, with the concentration of the N, Fe-CDs increasing, the absorbance of Rh B at 554 nm gradually decreases, indicating that Rh B was degraded by ·OH produced in the system, consistent with the results obtained by the EPR experiment. Therefore, it was speculated that the peroxidase catalytic of N, Fe-CDs was attributed to the formation of ·OH. In other words, N, Fe-CDs catalyze the decomposition of H_2O_2 to produce highly active intermediate ·OH, which oxidizes TMB into the green oxidation state ox-TMB [23]. The POD catalytic process of N, Fe-CDs is shown in Fig. 5.

Multifunction application of N, Fe-CDs based on the POD activity

Colorimetric detection of H_2O_2

Based on the POD activity of N, Fe-CDs, TMB was oxidated to ox-TMB in the presence of H_2O_2 and N, Fe-CDs. The oxidation of TMB was regulated by H_2O_2 concentration according to the previous literature [24]. Therefore, the color change caused by the TMB oxidation was utilized to realize the colorimetric detection of H_2O_2. As can be seen from Fig. 6A, with the increase of H_2O_2 concentration, the absorbance of ox-TMB at 652 nm gradually increases, and the color of the solution changes from colorless to green. Meanwhile, as shown in Fig. 6B, it has a good linearity in the concentration range of 1−100 μM. The detection limit calculated by the formula 3σ/s was 0.40 μM (S/N = 3), and the correlation coefficient R^2 was 0.9928. Table S2 compares the experimental results with nanocomposites and other CDs, and it was found that this result has a lower detection limit or a wider linear range. Therefore, a convenient and sensitive method to detect H_2O_2 based on the oxidation of TMB catalyzed by N, Fe-CDs was constructed.

Colorimetric detection of ascorbic acid

AA has reducibility and can reduce green ox-TMB to colorless TMB. Based on this, the colorimetric detection of AA can be realized. As shown in Fig. 6C, the absorbance of TMB at 652 nm decreases with the increase of AA concentration in the reaction system. The absorbance change of TMB was linearly correlated with AA concentration (5–50

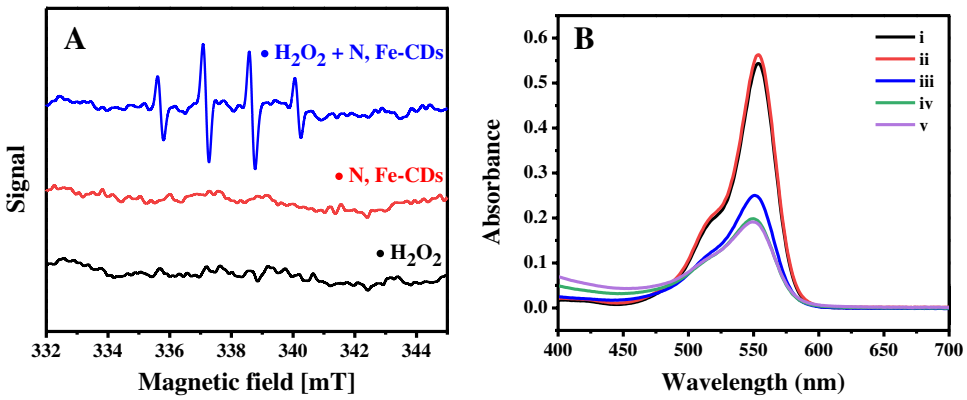

Fig. 4 **A** EPR spectra of ·OH radicals signal generated by the reaction of DMPO probe in H_2O_2, N, Fe-CDs, H_2O_2, and N, Fe-CDs system. **B** Absorption spectra of Rh B degradation in different reaction systems: (i) Rh B, (ii) Rh B + H_2O_2, (iii) Rh B + H_2O_2 + N, Fe-CDs (10 μg/mL), (iv) Rh B + H_2O_2 + N, Fe-CDs (30 μg/mL), and (v) Rh B + H_2O_2 + N, Fe-CDs (50 μg/mL). The concentrations of RhB and H_2O_2 are 50 μM and 0.5 mM, respectively

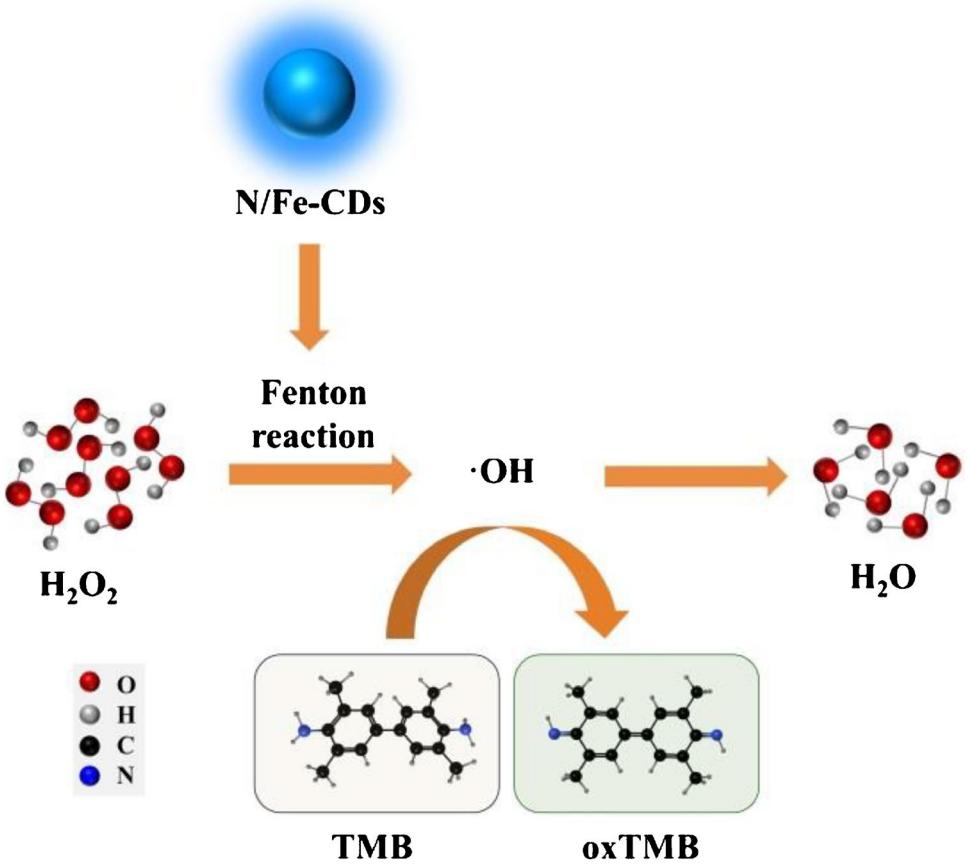

Fig. 5 Schematic diagram of the POD catalytic process of N, Fe-CDs

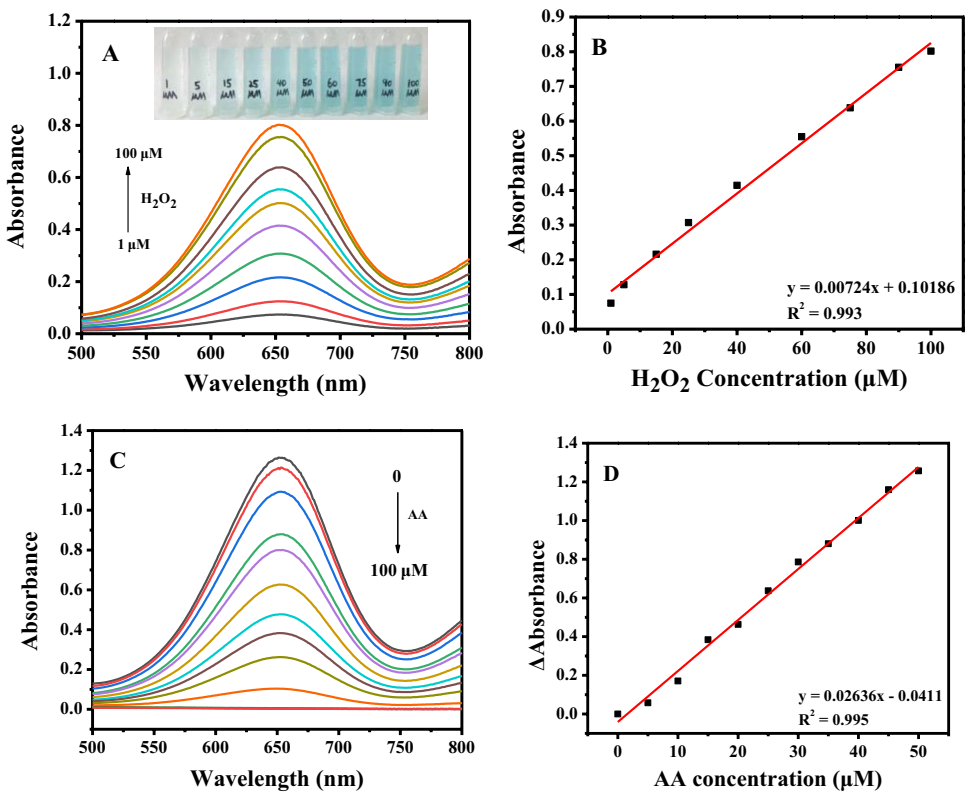

Fig. 6 **A** Absorption spectra of N, Fe-CDs-TMB solution on addition of various concentrations of H_2O_2 (1−100 μM). Insert of (**A**) showed the color of the corresponding solution. The concentrations of H_2O_2 (from left to right) are 1, 5, 15, 25, 40, 50, 60, 75, 90, and 100 μM, respectively. **B** Calibration curve of absorbance at 652 nm vs. concentration of H_2O_2. **C** Absorption spectra of N, Fe-CDs-TMB- H_2O_2 solution on addition of various concentrations of AA (0−100 μM). **D** The linear relationship between AA concentration and absorbance change. The error bars of (**B**) and (**D**) indicated the standard deviation of three experiments

μM), with correlation coefficient $R^2 = 0.9962$ (Fig. 6D), and the calculated detection limit was 2.05 μM. To evaluate the potential influence of some possible interference substances on the detection of AA, the absorbances of N, Fe-CDs-TMB-H_2O_2 system adding AA or different interferential substances were determined, respectively. The experimental results (Fig. S3) showed that the influence of these interference substances on AA detection was negligible under experimental conditions, indicating that our method has excellent specificity for AA detection. Table S3 shows the experimental results of AA detection by nanocomposites and other CDs using fluorescence and colorimetric methods. Compared with fluorescence methods, colorimetric techniques have certain limitations in the sensitivity and linear range, but have the advantages of stability and repeatability, which depend on the technique itself. However, compared with similar methods, this result has a lower detection limit. Therefore, N, Fe-CDs can be used as colorimetric probes for the detection of AA.

The AA concentration in fruit juice, vitamin C tablets, and human serum samples was determined to explore the actual availability of the sensing method. As shown in Table 1, the measured values in fruit juice and vitamin C tablets are very close to the labeled concentration. In addition, the results of recovery tests from 98.0 to 123.1%, and the RSD is satisfactory within 6%, indicating that the colorimetric probe has excellent potential for the detection of AA in actual samples.

Table 1 Results of measurement of AA in serum, food, and drug

Sample	Concentration (μM)		Recovery (%)	RSD ($n = 3$) (%)
	Added	Found		
Serum 1	20.0	20.5 ± 1.8	102.3	3.0
	40.0	49.2 ± 2.6	123.1	1.8
Serum 2	20.0	20.8 ± 3.6	104.2	5.7
	40.0	39.2 ± 5.2	98.0	4.4
Sample	Labeled concentration (mM)		Found concentration (mM)	
Fruit juice	5.68		5.71	
Vitamin C Tablets	5.70		5.72	

The protective effect of N, Fe-CDs on peroxidation of vascular smooth muscle cells damaged by H_2O_2

To determine the protective effect of N, Fe-CDs on the peroxidation of vascular smooth muscle cells (VSMCs), the cytotoxicity of N, Fe-CDs (25, 50, 100 μg/mL) to VSMCs was measured with CCK-8 assays (Fig. 7A) firstly. It was found that N, Fe-CDs could promote the growth and increase the viability of VSMCs with increasing concentration. Therefore, N, Fe-CDs had no cytotoxicity to VSMCs under the experiment concentrations.

H_2O_2 is one of the reactive oxygen species (ROS), which can cause oxidative stress and lead to cell damage. POD can convert H_2O_2 into non-toxic H_2O to protect cells from oxidative stress [25]. In Fig. 7B, the viability of VSMCs decreased by over 60% under 500 μM of H_2O_2 compared with the control. And the N, Fe-CDs could significantly increase the viability of VSMCs damage caused by H_2O_2. It demonstrated that N, Fe-CDs had a protective effect on the cell damage caused by H_2O_2.

Conclusion

In this work, the multifunctional N, Fe-CDs were successfully synthesized using a one-pot hydrothermal method. N, Fe-CDs with POD activity can catalyze the oxidation of the peroxidase substrate TMB to produce green ox-TMB in the presence of H_2O_2. On this basis, a colorimetric method with excellent linear detection range and low LOD for the detection of H_2O_2 and AA was established. Subsequently, this method has been used successfully for the determination of AA in actual samples, suggesting its potential application in the food field and clinical testing. In addition, cell viability

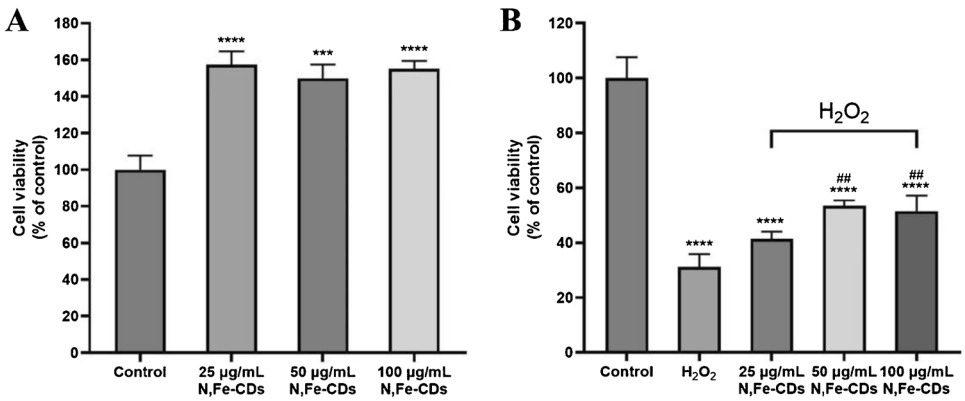

Fig. 7 Cell viability of CCK-8 assays: **A** VSMC cells were incubated with N, Fe-CDs (25, 50, and 100 μg/mL) for 24 h (data = mean ± SD; $n = 6$). ***$P < 0.001$ and ****$P < 0.0001$ compared to controls. **B** VSMC cells were incubated with N, Fe-CDs (25, 50, 100 μg/mL) and H_2O_2 (500 μM) for 24 h (data = mean ± SD; $n = 6$). ****$P < 0.0001$ compared to controls; $^{\#\#}P < 0.01$ vs. H_2O_2 treatment group

experiments illustrated that N, Fe-CDs had a protective effect on the cell damage caused by H_2O_2. This study has promising prospects for application in food fields, biochemistry, and cell antioxidant protection.

Supplementary information The online version contains supplementary material available at https://doi.org/10.1007/s00604-024-06456-4.

Author contribution Material preparation and characterization were carried out by R.L. and M.F. POD activity was tested by Y.L. The cell culture and experiments were carried out by B.Z. and Y.T. Data collection and analyses were performed by Y.L. The first draft of the manuscript was written by S.C., and the check of the manuscript was done by L.G. All authors read and approved the final manuscript.

Funding This work is completed with funding from the National Natural Science Foundation of China (31201305), the Natural Science Foundation of Hebei Province (B2019205054, B2021205001), and the Science Foundation of Hebei Normal University (L2020B07, L2023J01).

Data availability All data that support the findings of this study are included within the article and any supplementary files.

Declarations

Ethical approval This research did not involve human or animal samples.

Conflict of interest The authors declare no competing interests.

References

1. Jiang D, Ni D, Rosenkrans ZT, Huang P, Yan X, Cai W (2019) Nanozyme: new horizons for responsive biomedical applications. Chem Soc Rev 48(14):3683–3704. https://doi.org/10.1039/c8cs00718g
2. Chen Y, Cao H, Shi W, Liu H, Huang Y (2013) Fe-Co bimetallic alloy nanoparticles as a highly active peroxidase mimetic and its application in biosensing. Chem Commun (Camb) 49:5013–5015. https://doi.org/10.1039/c3cc41569d
3. Zhang X, Lin S, Liu S, Tan X, Dai Y, Xia F (2021) Advances in organometallic/organic nanozymes and their applications. Coordin Chem Rev 429:213652. https://doi.org/10.1016/j.ccr.2020.213652
4. Zhu D, Zhuo S, Zhu C, Zhang P, Shen W (2019) Synthesis of catalytically active peroxidase-like Fe-doped carbon dots and application in ratiometric fluorescence detection of hydrogen peroxide and glucose. Anal Methods 11(20):2663–2668. https://doi.org/10.1039/c9ay00342h
5. Liang M, Yan X (2019) Nanozymes: from new concepts, mechanisms, and standards to applications. Acc Chem Res 52:2190–2200. https://doi.org/10.1021/acs.accounts.9b00140
6. Ju J, Chen W (2015) In situ growth of surfactant-free gold nanoparticles on nitrogen doped graphene quantum dots for electrochemical detection of hydrogen peroxide in biological environments. Anal Chem 87:1903–1910. https://doi.org/10.1021/ac5041555
7. Kan X, Liu J, Chen Y, Guo W, Xu D, Cheng J, Cao Y, Yang Z, Fu S (2021) Myricetin protects against H_2O_2-induced oxidative damage and apoptosis in bovine mammary epithelial cells. J Cell Physiol 236(4):2684–2695. https://doi.org/10.1002/jcp.30035
8. Gao X, Zhou X, Ma Y, Qian T, Wang C, Chu F (2019) Facile and cost-effective preparation of carbon quantum dots for Fe^{3+} ion and ascorbic acid detection in living cells based on the on-off-on fluorescence principle. Appl Surf Sci 469:911–916. https://doi.org/10.1016/j.apsusc.2018.11.095
9. Malik M, Narwal V, Pundir CS (2022) Ascorbic acid biosensing methods: a review. Process Biochem 118:11–23. https://doi.org/10.1016/j.procbio.2022.03.028
10. Bhunia SK, Dolai S, Sun H, Jelinek R (2018) On/off/on hydrogen-peroxide sensor with hemoglobin-functionalized carbon dots. Sens Actuators B Chem 270:223–230. https://doi.org/10.1016/j.snb.2018.05.029
11. Chen B, Wang F, Yao W, Lin Z, Zhang X, Luo S, Zheng L, Lin X (2018) Carbon Nitride quantum dot-enhanced chemiluminescence of hydrogen peroxide and hydrosulfite and its application in ascorbic acid sensing. Anal Methods 10(4):474–480. https://doi.org/10.1039/c7ay02777j
12. Cao L, Zan MH, Chen FM, Kou X, Liu Y, Wang P, Mei Q, Zou Z, Dong W, Li L (2022) Formation mechanism of carbon dots: from chemical structures to fluorescent behaviors. Carbon 194:42–51. https://doi.org/10.1016/j.carbon.2022.03.058
13. Ni T, Li Q, Yan Y, Wang F, Cui X, Yang Z, Wang Y, Yang Z, Chang K, Liu G (2020) N, Fe-doped carbon dot decorated gear-shaped WO_3 for highly efficient UV-Vis-NIR-driven photocatalytic performance. Catalysts 10(4):416. https://doi.org/10.3390/catal10040416
14. Liu Y, Xu B, Lu M, Li S, Guo J, Chen F, Xiong X, Yin Z, Liu H, Zhou D (2021) Ultrasmall Fe-doped carbon dots nanozymes for photoenhanced antibacterial therapy and wound healing. Bioact Mater 12:246–256. https://doi.org/10.1016/j.bioactmat.2021.10.023
15. Wang C, Shi H, Yang M, Yan Y, Liu E, Ji Z, Fan J (2020) Facile synthesis of novel carbon quantum dots from biomass waste for highly sensitive detection of iron ions. Mater Res Bull 124:110730. https://doi.org/10.1016/j.materresbull.2019.110730
16. Ci Q, Wang Y, Wu B, Coy E, Li JJ, Jiang D, Zhang P, Wang G (2023) Fe-doped carbon dots as NIR-II fluorescence probe for in vivo gastric imaging and pH detection. Adv Sci 10(7):e2206271. https://doi.org/10.1002/advs.202206271
17. Li Q, Lu H, Wang X, Hong Z, Fu Z, Liu X, Zhou J (2022) Visible-light-driven N and Fe co-doped carbon dots for peroxymonosulfate activation and highly efficient aminopyrine photodegradation. Chem Eng J 443:136473. https://doi.org/10.1016/j.cej.2022.136473
18. Liu YS, Luo S, Wu P, Ma C, Wu X, Xu M, Li W, Liu S (2019) Hydrothermal synthesis of green fluorescent nitrogen doped carbon dots for the detection of nitrite and multicolor cellular imaging. Anal Chim Acta 1090:133–142. https://doi.org/10.1016/j.aca.2019.09.015
19. Zhang Y, Wang YN, Sun XT, Chen L, Xu ZR (2017) Boron nitride nanosheet/CuS nanocomposites as mimetic peroxidase for sensitive colorimetric detection of cholesterol. Sens Actuators B Chem 246:118–126. https://doi.org/10.1016/j.snb.2017.02.059
20. Xi X, Peng X, Xiong C, Shi D, Zhu J, Wen W, Zhang X, Wang S (2020) Iron doped graphitic carbon nitride with peroxidase like activity for colorimetric detection of sarcosine and hydrogen peroxide. Microchim Acta 187(7):383. https://doi.org/10.1007/s00604-020-04373-w
21. Das S, Ngashangva L, Mog H, Gogoi S, Goswami P (2021) An insight into the mechanism of peroxidase-like activity of carbon dots. Opt Mater 115:111017. https://doi.org/10.1016/j.optmat.2021.111017
22. Li P (2022) The valine-based N-doped carbon dots with high peroxidase-like activity. Luminescence 37(10):1725–1732. https://doi.org/10.1002/bio.4348

23. Wang B, Chen Y, Wu Y, Weng B, Liu Y, Li CM (2016) Synthesis of nitrogen-and iron-containing carbon dots, and their application to colorimetric and fluorometric determination of dopamine. Microchim Acta 183:2491–2500. https://doi.org/10.1007/s00604-016-1885-5
24. Singh VK, Yadav PK, Chandra S, Bano D, Talat M, Hasan SH (2018) Peroxidase mimetic activity of fluorescent NS-carbon quantum dots and their application in colorimetric detection of H_2O_2 and glutathione in human blood serum. J Mater Chem B 6(32):5256–5268. https://doi.org/10.1039/c8tb01286e
25. Kong B, Yang T, Cheng F, Qian Y, Li C, Zhan L, Li Y, Zou H, Huang C (2022) Carbon dots as nanocatalytic medicine for anti-inflammation therapy. J Colloid Interface Sci 611:545–553. https://doi.org/10.1016/j.jcis.2021.12.107